Florian Böhmermann, Oltmann Riemer

Development and application of a test rig for tribological investigations under impact loads

Recommended Citation (primary publication/Version of Record) incl. DOI:

Florian Böhmermann, Oltmann Riemer,
Development and application of a test rig for tribological investigations under impact loads,
CIRP Journal of Manufacturing Science and Technology,
Volume 19, 2017, Pages 129-137, ISSN 1755-5817,
https://doi.org/10.1016/j.cirpj.2017.07.004.
(https://www.sciencedirect.com/science/article/pii/S1755581717300391)

Development and application of a test rig for tribological investigations under impact loads

Florian Böhmermann*, Oltmann Riemer

LFM Laboratory for Precision Machining, University of Bremen, Badgasteiner Straße 2, 28359 Bremen, Germany

A R T I C L E   I N F O

A B S T R A C T

The investigation and the understanding of frictional mechanisms occurring between forming dies and work pieces in tribological contact is the prerequisite for the development of novel, dry bulk metal forming processes such as dry rotary swaging. The capability to conduct tribological investigations within the actual forming processes, however, is strongly limited, e.g. due to the limited accessibility of force measurement equipment. This work presents the development and application of a tribological test rig mimicking typical contact geometries and high impact loads associated with infeed rotary swaging for process-independent tribological investigations. The development comprises the designing process based on rotary swaging process simulations, setup assembly, and calibration procedure. Subsequently, the functionality of the test rig was demonstrated successfully, determining the distinct frictional properties under lubricated and dry conditions of various samples with structured surfaces representative for rotary swaging dies.

© 2017 CIRP.

Introduction

Cold bulk metal forming processes are a key technology for the economic mass manufacture of metallic components. These processes are commonly associated with high pressures per unit area between forming dies and work pieces, resulting in considerably high frictional shear stresses in the forming zone. These extreme conditions require the use of lubricants in order to protect the forming dies from abrasive and adhesive wear as well as to provide desired work piece quality. With regard to economic and ecological benefits, the lubricant free, thus, dry performance of cold bulk metal forming processes is considered to be highly innovative [1].

A first approach towards a dry process layout in cold bulk metal forming was shown for infeed rotary swaging [2]. Here, the functionalities of the lubricant are substituted by functionalized forming dies exhibiting diamond like carbon (DLC) hard coatings and structured surfaces [3]. The hard coatings are applied as wear protection for the rotary swaging dies and should furthermore avoid the generation of abrasive particles form the work pieces by providing favorable tribological, low friction conditions, whilst the

structured surfaces are used to control the process forces, i.e. the axial reaction force.

Even though first dry infeed rotary swaging experiments with functionalized forming dies were carried out successfully, the fundamental effects of coatings and structures on the frictional properties of die surfaces, especially under impact loads typical for rotary swaging, are still not fully understood [4]. More comprehensive tribological investigations are necessary to build up the knowledge for the development of robust dry rotary swaging processes applied on an industrial scale. However, such investigations cannot be easily carried out within actual infeed rotary swaging. This is due to the strongly limited accessibility to e.g. force measurement equipment and in practice requires the manufacture of a new set of rotary swaging dies for every new experimental design [5]. Common techniques for tribological investigations with regard to bulk metal forming – these are namely the cylinder compression test and the ring compression test – could be applied [6]. However, those setups do not reflect typical impact loads and the achievable strain rates are considerably lower than in real rotary swaging.

In this work a new test rig for tribological investigations under impact loads was developed and applied. This test rig mimics typical contact geometries of infeed rotary swaging dies and work pieces and allows for the application of variable impact loads to the samples. The frictional properties of e.g. structured or hard coated forming die samples can be evaluated by the indirect measurement

* Corresponding author.
  E-mail address: boehmermann@lfm.uni-bremen.de (F. Böhmermann).

of the maximum horizontal reaction force resulting from the impact. This particular design allows the relative motion in between the forming die sample and the work piece sample, reflecting the conditions of the actual process. After completing the setup, investigations of the tribological properties of multiple forming die samples exhibiting structured surfaces with various designs were performed under lubricated and dry conditions. Here, the functionality of the test rig was demonstrated successfully. Furthermore, it was found that structured surfaces notably change the frictional conditions under impact loads and are a promising approach for friction control in dry bulk metal forming.

Rotary swaging fundamentals

Rotary swaging is a cold bulk metal forming process with widespread use, particularly in the automotive industry. Typical products are axles or steering spindles made from rods or hollow shafts. Work pieces machined by rotary swaging exhibit considerably improved material properties, compared to those machined by cutting processes. This is due to strain hardening induced by the manufacturing process and undisturbed material fiber flow. Furthermore, the flexible adjustment of work piece's wall thicknesses allows the best material utilization and consequent light weight design. In infeed rotary swaging the work piece is axially feed into the swaging unit and incrementally reduced in its diameter by the repetitive strokes of the forming dies, what can be considered as impact loads. The contact time of dies and work pieces, here, hardly exceeds $500\,\mu s$. The imposed radial forming force F_R directly emerges in an axial reaction force F_A counteracting the feed force F_f. The magnitude of the axial reaction force is determined by the forming die's geometry – here the forming die angle α in the reduction zone – and the frictional conditions between work pieces and dies in tribological contact. Typical for cold bulk metal forming processes, rotary swaging is characterized by significantly high pressures per unit area between forming dies and work pieces making the use of lubricant essential to gain a robust process layout [7]. The lubricant protects the forming dies from abrasive and adhesive wear, provides geometrical accuracy and suitable surface finish of the work pieces, and purges abrasive particles from the swaging unit [8]. The use of lubricants, however, leads to a considerably increased axial reaction force F_A. Therefore, commercially available rotary swaging dies exhibit a rough layer of thermally sprayed tungsten carbide with cobalt binder phase (WC-Co) in the reduction zone. This layer helps to increase the effective friction between rotary swaging dies and the work piece and, thus, reduces the axial reaction force. The principle of infeed rotary swaging including all relevant geometries and forces is shown in Fig. 1.

Structured forming die surfaces

The texture or structures of a surface significantly influences its tribological performance, i.e. decrease or increase friction. This allows the application of structured surfaces to forming dies for the control of process forces, e.g. through affecting the material flow. The functionality of surface structures is primarily related to their geometrical dimensions: microscopic, mesoscopic and macroscopic. Microscopic structures, such as pockets with a depth of several micrometers, can serve as lubricant reservoirs to achieve hydrodynamic separation of forming dies and work pieces and, thus, reduce friction and wear. This effect was demonstrated by Popp and Engel for a micro textured punch machined by laser ablation for backward can extrusion. The punch exhibited circular shaped pockets with a targeted width and depth of $10\,\mu m$ and $1\,\mu m$, respectively. Compared to the machining results achieved with a non-structured punch, the forming die life was increased by
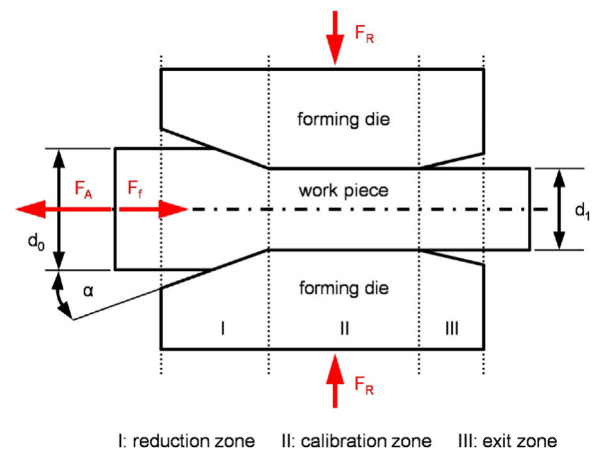

Fig. 1. Cross sectional illustration of the infeed rotary swaging process.

approximately 50% [9]. Arentoft et al. presented samples exhibiting a $5\,\mu m$ thick layer of a sponge like surface structure that can serve as a lubricant carrier. Such surfaces were generated by first the electrochemical deposition of the immiscible alloy SnZn and the subsequent etching of the Zn phase leaving the desired porous micro structure. The tribological effectiveness of such structured samples was investigated in ring compression and double cup extrusion tests. Significantly lower friction and an increased resistance against galling were achieved when applying such structured surfaces together with low viscous mineral oil as lubricant compared to the results with non-coated samples [10]. Furthermore, micro structures or textures, preferably characterized by areal roughness parameters according to ISO 25178 standard, can reduce friction under dry conditions. Brinksmeier et al. showed the capability of periodic micro structured sample surfaces generated by micro milling to reduce friction in tribological contact. Samples from 1.2379 hardened tool steel were manufactured and tested against 1.4301 austenitic stainless steel sheets in dry strip drawing tests. Compared to polished references, a 20% reduced coefficient of friction was found for selected micro structured samples [11]. The findings later were underlined by Böhmermann and Riemer using a micro tribometer in ball-on-plate configuration [12]. The results were explained by some ideal tribological conditions provoked by the micro milled surface leading to a low coefficient of friction. This is first: a distinctively reduced real area of contact between the surfaces in tribological contact and, thus, a reduction of adhesive friction. Secondly: the micro structure's design can generally be characterized as smooth and is able to suppress the formation of cutting type wear under given conditions – this is the applied pressure per unit area and the drawing speed – as introduced by Kayaba et al. [13]. Micro structured surfaces, furthermore, are able to maintain low coefficients of friction under dry conditions by entrapping wear particles generated during the tribological contact. Such particles, otherwise, would lead to an increase of friction in dependence on the sliding length due to plowing or three body deformation. Suh and Saka presented pin-on-disk tribological investigations applying flat and undulated surfaces (structure height $50\,\mu m$, structure width $100\,\mu m$) from copper generated by photo-lithography and electro-etching. Undulated surfaces constantly provoked low coefficients of friction of about 0.2 even for sliding distances greater than $50\,m$ due to the capability of entrapping wear debris, while that for the flat surface increased by 400% [14].

Mesoscopic structures, i.e. grooves with the size of some ten to a few hundreds of micrometers, can be applied to conventional sheet metal forming to control the material flow. Franzen et al. introduced samples for strip drawing tests exhibiting grooves

machined by deep rolling. The deep rolling tool applied was 13 mm in diameter; the targeted groove depth was 6.5 μm, the resulting groove width approximately 900 μm. Those structured surfaces allowed to distinctively increase friction due to additional elastic deformation of the work piece material in contact with the forming die samples associated with higher friction [15].

Structures of larger feature size – 100 μm and above – are referred as macroscopic structures. Common examples for such structures are drawbeads applied in forming of complex shaped sheet metal work pieces such as car body parts. Main function of drawbeads is the control of the material flow due to additional bending operations and an increased area of contact between the forming die and the sheet metal, both associated with an increase of friction [16]. Brosius and Mousavi presented a concept utilizing structured die surfaces for dry deep drawing. Dies and blank holders applied exhibited macroscopic structures arranged concentrically around the drawing cavity. The structures considerably reduced the area of contact with the sheet metal and, thus, the required blank holder force. Compared to conventional deep drawing with unstructured dies, the contact pressure per unit area between die and work piece was fundamentally reduced, enabling the conduction of deep drawing experiments under dry conditions [17]. Hermann et al. used rotary swaging dies exhibiting macro structured reduction zones for process forces control [18]. In comparison to unstructured rotary swaging dies, this novel die design allowed to reduce the tracking error of the feed system associated with the axial reaction force by 50% for dry forming and up to 400% when forming under lubricated conditions. The functionality of such macroscopic structures in bulk metal forming is based on their imprinting into the softer work piece material. The imprinting provokes an increase of the real area of contact and an interlocking of forming dies and work piece. When maintaining the forming operation, a shift of the friction mechanism from slip between both the surfaces towards shearing of the softer work piece material generally associated with higher friction occurs, compare Ref. [19]. The effectiveness of macroscopic structures influencing friction is mainly determined by greater overall heights, an increased height to width ratio, and the alignment of the structures relatively to the material flow in the forming operation. However, more distinct structures can negatively affect the machining results, e.g. increase the surface roughness of the work piece.

Tribological test rig

Background

An infeed rotary swaging process should exemplary represent the basis for the development of the tribological test rig. The swaging unit comprises four rotary swaging dies. The dies applied should exhibit a forming die angle of $\alpha = 10°$ and allow a diameter reduction of rods and hollow shafts from $d_0 = 20$ mm down to $d_1 = 15$ mm. These constraints result in an area of contact of $A = 198.383$ mm^2 for each of the four rotary swaging dies and the work piece within the die's reduction zone, compare Fig. 2.

Layout and design of the tribological test rig's components presume the sufficient estimate of necessary excitation forces, i.e. the radial forming force F_R and related pressures per unit area, respectively. Finite element modelling and simulation should be applied to derive the required information. Here, a two-dimensional axes-symmetric model of the exemplary rotary swaging process was introduced [20]. The rotary swaging dies were implemented as rigid bodies; work pieces were implemented as rods with the mechanical properties of 1.4301 (X5CrNi18-10) austenitic stainless steel. A coefficient of friction of $\mu = 0.5$ according to Coulomb's friction model was predetermined for dies and work pieces in tribological contact. For all simulations, the stroke height of the forming dies and the swaging
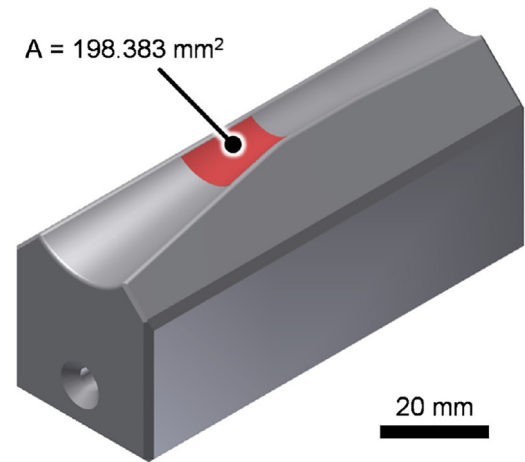

Fig. 2. 3D-sketch of one single forming die of the exemplary infeed rotary swaging process for the diameter reduction of rods and hollow shafts from 20 mm to 15 mm. The contact area A of die and the work piece within the reduction zone is marked in red (For interpretation of the references to color in this figure legend, the reader is referred to the web version of this article.).

frequency were kept constant at $h_t = 1$ mm and $f_s = 37.5$ Hz respectively, whilst the feed velocity was varied in a range of $v_f = 120$ mm/min to 3000 mm/min. The maximum radial forging force F_R emerging at one rotary swaging die during the forming stroke was determined from the simulation for the condition that both the reduction zone and the calibration zone of the die make full contact with the work piece. Depending on the preset feed velocity, the radial forging force was found to be in the range of 319.8 kN–454.4 kN. The contact time of dies and the work piece during one stroke increased towards higher feed velocities from $t = 140$ μs to 560 μs. The resulting pressures per unit area p_s within the reduction zone of the forming dies in dependence on the feed velocity were calculated according to Eq. (1) with $p_s = 1587.3$ N/mm^2–2255.7 N/mm^2.

$$p_s = \frac{F_R \cos \alpha}{A} \tag{1}$$

A differentiated consideration of pressure per unit area for the reduction and the calibration zone was neglected at this point, as the proportion of the radial forming force F_R resulting from the contact of the forming dies and the work piece within the calibration zone is estimated to be considerably lower than that resulting from the forming operation within the reduction zone.

Design

Main functions of the tribological test rig are the application of variable impact loads to a forming die sample and a work piece sample in tribological contact as well as the measurement of the excitation force $F_{R'}$, correlating with the radial forming force F_R in rotary swaging, and the emerging maximum horizontal reaction force $F_{A'}$, correlating with the axial reaction force F_A. Some principal constraints regarding the engagement and the size of the samples should be highlighted at this point, before further introducing the test rig's design. As in the exemplary rotary swaging process, the samples should be engaged under an angle of 10°; the forming die samples should be of simple design with planar surface that should exhibit the characteristics of functionalized rotary swaging dies, i.e. structures and hard coatings; the area of contact between the forming die sample and work piece sample in tribological contact should be limited to 100 mm^2. The latter is seen to be a good compromise between the representation of the actual contact of one rotary swaging die and the work piece

within the reduction zone and the limitation of the magnitude of the required impact.

With regard to simplicity and repeatability a guided falling mass should be used for the application of the excitation force $F_{R'}$. The maximum drop height, here, should not exceed $h_{max} = 1$ m. According to the simulation results the mechanism must be able to apply a maximum momentary pressure per unit area of 2255.7 N/mm² to the samples in tribological contact. This corresponds to a maximum excitation force $F_{R'}$ of 229.0 kN for the area of contact of 100 mm². The necessary falling mass can be determined according to the following procedure starting with Newton's second law of motion, stating that the net force on an object is equal to the change in momentum.

$$F = m\,a = m\frac{dv}{dt} = \frac{dp}{dt} \qquad (2)$$

The change in momentum or impulse I can be calculated bringing the equation in the form:

$$\Delta p = I = \int_{t_1}^{t_2} F(t)dt \qquad (3)$$

For the constraint that the force F acting on the object should be constant within the time interval $[t_1, t_2]$ Eq. (3) can be simplified to:

$$\Delta p = I = m\,\Delta v = F\Delta t \qquad (4)$$

in which Δt is the contact time where the force F is acting. The velocity of an object accelerated by gravity can be calculated in dependence on the drop height h or h_{max} in the particular case according to Eq. (5)

$$v = \sqrt{2\,g\,h} = \sqrt{2\,g\,h_{max}} \qquad (5)$$

With the assumption, that the falling mass comes to an immediate rest after the impact, the change in velocity Δv equals the velocity v and the necessary mass can be calculated from Eq. (4) according to:

$$m = \frac{F\Delta t}{v} \qquad (6)$$

For the calculation, here, the estimation of the contact time Δt is required. For the elastic collision of steel made objects the contact time usually does not exceed a few hundred micro seconds, where the mass and the rigidity of the impacting body predominantly determine the results [21]. With an estimated contact time of 1000 μs the maximum falling mass for the tribological test rig was calculated to 51.7 kg according to Eq. (7).

$$m = \frac{229.0\,\text{kN}\cdot 0.001\,\text{s}}{4.43\,\text{s}} = 51.7\,\text{kg} \qquad (7)$$

An illustration of the final setup of the test rig for tribological investigations under impact loads is shown in Fig. 3. The mechanism for the application of the excitation force $F_{R'}$ is implemented as a two column guided traverse including a hammer impacting on the sample holder arrangement. Traverse and hammer together have a mass of m = 21 kg that can be extended to up to 60 kg by supplemental weights. The actual excitation force $F_{R'}$ is determined by direct force measurement using a pre-stressed Kistler 9091A piezo-electric force transducer. The force transducer is embedded in the 500 mm by 500 mm base plate and carries the sample holder arrangement. The sensitivity of the force transducer is given by the manufacturer with 20 mN; the measurement range with 0 kN to 1200 kN for dynamic compressive forces. Besides the force transducer, the measurement chain comprises a Kistler 5019 multichannel charge amplifier as well as a computer equipped with an I/O A/D converter card for data sampling.
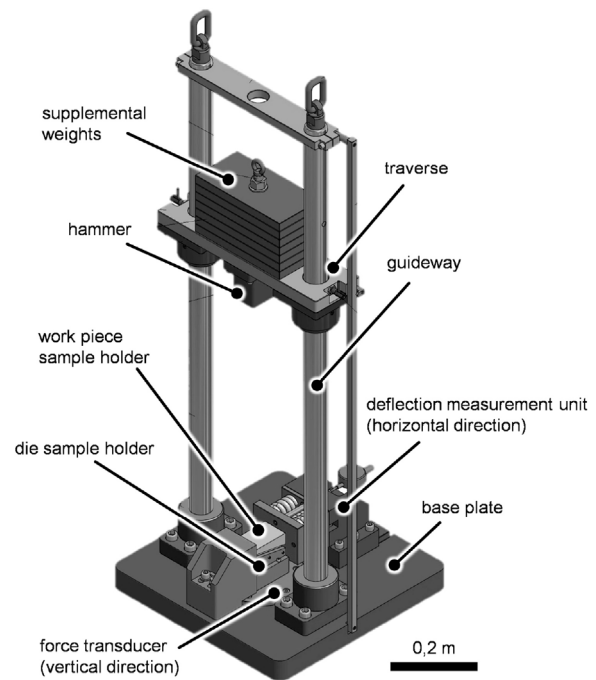

Fig. 3. Illustration of the tribological test rig (in accordance with Ref. [22]).

The forming die sample and the work piece sample are embedded in tailor-made cavities in the associated sample holders using no additional fixtures. The forming die sample is a cuboid with 30 mm by 15 mm tribologically active top surface. The work piece sample is characterized by an area of 20 mm by 5 mm (100 mm²) that is in tribological contact with the die sample. The longitudinal sides of the samples, here, should coincide with the feed direction – this is the axial direction – of infeed rotary swaging. Both the sample holders are engaged under an angle of 10° representing the contact conditions of the rotary swaging dies and the work piece within the reduction zone. This arrangement enforces a horizontal relative movement of the work piece sample holder directly acting against the deflection measurement unit once an excitation force $F_{R'}$ in vertical direction is applied. Additional guideways alongside the forming die sample holder prevent from a relative movement other than the longitudinal direction of the samples. A detailed view of the forming die sample holder, the work piece sample holder, and their arrangement is given in Fig. 4.

The tribological test rig allows for the indirect measurement of the maximum horizontal reaction force $F_{A'}$ by recording the maximum compression of a column guided spring assembly caused by the horizontal relative movement of the work piece sample holder. The magnitude of the compression force acting on the spring assembly is directly determined by the frictional conditions between both the samples. In comparison to a direct force measurement in horizontal direction, this design allows the relative motion between the forming die sample and the work piece sample, reflecting the conditions of the actual rotary swaging process. A detailed illustration of the deflection measurement unit for indirect force measurement is given in Fig. 5. The unit comprises of up to five spiral springs, each with a spring rate of 2045 N/mm, and a 10 mm range precision dial with drag indicator for recording the maximum compression of the spring assembly during the experiment.

Calibration

Before applying the test rig in tribological investigations, a calibration procedure was carried out to determine the actual
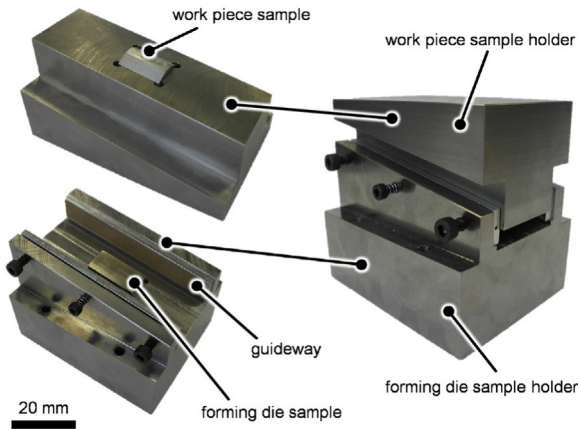
Fig. 4. Forming die sample holder and work piece sample holder and their arrangement under an engagement angle of 10°.

excitation force $F_{R'}$ that can be generated by the guided falling mass in dependence on the drop height h. For this procedure the sample holders were arranged as in the setup for tribological investigation but without samples. Additionally, the work piece sample holder was blocked to prevent sliding towards the deflection measurement unit. The area of contact between the two sample holders in this configuration was about 3000 mm². This resulted in a considerably low pressure per unit area and only elastic deformations of the components when an excitation force was applied. The embedded force transducer was used for the measurement of the excitation force; the sampling rate was 50 kHz. No supplemental weights were used for the calibration procedure. The drop height h of the traverse was varied in the range of 50 mm–300 mm. The maximum of the excitation force $F_{R'}$ and the contact time Δt, i.e. the width of the force peak, were determined form the force measurement signal by graphical analysis, compare Fig. 6.

Fig. 7 shows the measured excitation force $F_{R'}$ and contact time Δt in dependence on the drop height h. The contact time remains nearly invariant for every calibration experiment and averages to 0.25 ms, four times less than the anticipated contact time of 1 ms. This allows to operate the test rig with significantly lower drop heights and less supplemental weights then expected to obtain desired excitation forces $F_{R'}$ and pressures per unit area p_s, respectively.

A regression analysis was carried out for all ordered pairs of drop height h and excitation force $F_{R'}$ obtained from the calibration procedure, assuming a radix dependency. The result is displayed in Fig. 7. The required drop height h for the application of a predetermined excitation force $F_{R'}$ using the test rig can be calculated according to Eq. (8) derived from the
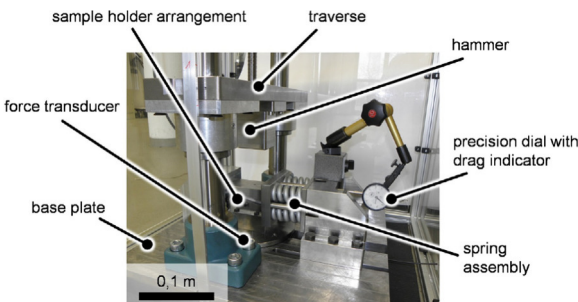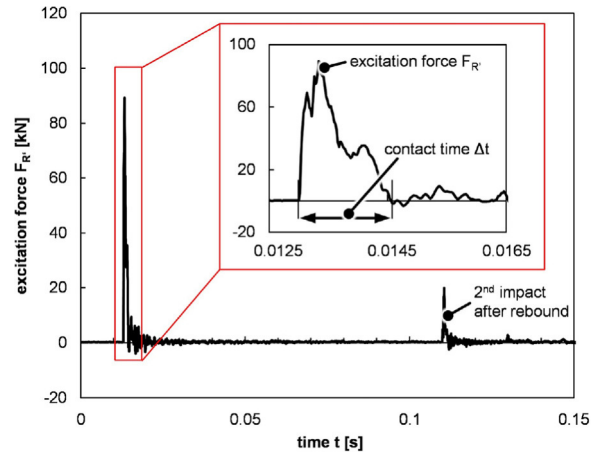

Fig. 6. Exemplary force signal of the excitation force $F_{R'}$ measured in calibration experiment for a drop height of the mass of 100 mm.

regression analysis.

$$h = \left(\frac{F_{R'}}{561945\frac{kg}{s^2}} \right)^{1.38} \tag{8}$$

Experimental section

Samples

Seven forming die samples exhibiting different surface structures were manufactured of 1.2379 (X153CrMoV12) hardened tool steel with a hardness of 60 ± 0.6 HRC. The generation of the sample's structured, tribological active 30 mm by 15 mm top surfaces was carried by micro milling using a DMG Sauer Ultrasonic 20 linear machine tool. Lubricant was applied during the machining operation. The general machining strategy remained unchanged for all samples. Micro ball-endmills of 1 mm in diameter were applied, the tool alignment was normal to the machined surfaces. The direction of feed was perpendicular to the longitudinal direction of the samples and the machining strategy was down milling. The process parameter depth of cut, width of cut, the feed velocity, and the spindle speed were kept constant at a_p = 0.03 mm, a_e = 0.05 mm, v_f = 3000 mm/min, and n = 35,000 min⁻¹ respectively. The first sample (#1) had a flat top surface. Nevertheless, on microscopic level, this sample exhibited periodic micro structures, which were generated by the particular engagement conditions of the tool and the work piece in micro

Fig. 5. Deflection measurement unit for the indirect measurement of the maximum horizontal reaction force $F_{A'}$.
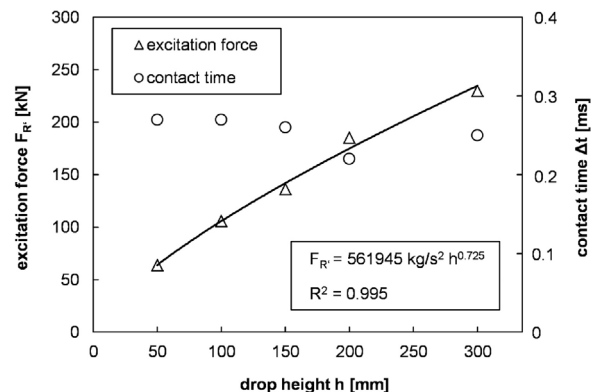

Fig. 7. Excitation force $F_{R'}$ (with non-linear regression curve) and contact time Δt in dependence on the drop height h of the traverse (m = 21 kg).

milling. The design of such micro structures is determined by the hardness of the machined material, the diameter of the tool, the feed per tooth, and the width of cut [23]. The sample #1 should be referred as the "microscopic" sample. The samples #2a, #2b, and #2c exhibited the same microstructured flat top surfaces as sample #1 but with additional grooves aligned perpendicular to the longitudinal direction of the samples. The targeted depth of the grooves was 50 µm. The groves were machined using a d = 0.2 mm diameter micro ball-endmill, the machining parameter were depth of cut a_p = 0,005 mm, feed velocity v_f = 1000 mm/min, and spindle speed n = 40,000 min^{-1}. The groove pitch was varied for the tree samples at 1.5 mm, 1.0 mm, and 0.5 mm. These samples should be referred as the "mesoscopic" samples. Subsequently, three samples with "macroscopic" structures were machined (#3a, #3b, #3c) using the same tool type and process parameters as before. Those samples exhibited sinewave structures each of λ = 1.3 mm in wavelength but with three different amplitudes A = 0.03 mm, 0.04 mm, and 0.05 mm. Photographs and attributed surface plots of three selected forming die samples exhibiting various surface structures are shown in Fig. 8. Additionally to the structured samples, one polished forming die sample (R) was manufactured, serving as a reference in the tribological investigations.

The work result was analyzed by means of optical metrology for roughness measurement and groove depth evaluation (mesoscopic structures only). A Sensofar Plu 2300 confocal profilometer with 50× magnification objective (vertical resolution 3 nm, lateral resolution 100 nm) was applied. The raw data was processed by an image processor (Scanning Probe Image Processor, SPIP^{TM}) to derive areal roughness parameters according to ISO 25178 standard. The primary profile was low-pass filtered using λ_s = 0.25 µm cut-off for noise removal and high pass filtered using λ_c = 0.08 mm cut-off for roughness/waviness separation. Additionally, for the macroscopic samples shape accuracy achieved was measured using the same confocal profilometer with a 20× magnification objective (vertical resolution 8 nm, lateral resolution 1.65 µm). For all samples the determined maximum height deviation of the sinewave structures amounted to 3 µm, the maximum deviation in structure width, i.e. the wavelength, amounted to 6 µm. An overview of all samples and the results of their surface's structure investigations are given in Table 1. The roughness values Sa are the average of three subsequent measurements, each taken on different spots on the sample. Besides it was found, that the actual groove depth for all the mesoscopic samples (#2a, #2b, and #2c) undershoot the targeted depth of 50 µm; for the sample #2c the average groove depth amounted only 18.6 µm.

Tribological investigation

The work piece samples for the tribological investigations were made from 1.0038 construction steel; a typical material for automotive components machined by rotary swaging. Before every experiment, the forming die samples and the work piece samples were thoroughly cleaned by rinsing and wiping using isopropyl alcohol. A new work piece sample was applied for every experiment. An experiment comprised of two strokes applied to the samples using the guided falling mass. This procedure enabled to reflect both, the tribological conditions of the first contact of the samples and a later state of the tribological system, where the surface structures of the forming die sample are already imprinted into the surfaces of the work piece sample. A drop height of 160 mm of the guided falling mass was selected for the experiments. This resulted in a nominal excitation force $F_{R'}$ of 148.8 kN, which corresponds to pressure per unit area of 1465.7 N/mm^2 acting on the samples during the experiments. Whilst every stroke the actual force in excitation direction $F_{R''}$ was measured using the piezo-electric force transducer embedded in the test rig's base plate. This force is expected to be less than the nominal excitation $F_{R'}$, due to the transfer of the impact's energy to forming work applied to the work piece sample. The maximum horizontal reaction force $F_{A'}$ was calculated after every experiment from the maximum compression of the column guided spring assembly recorded by the precision dial with drag indicator. Every experiment was carried out lubricated and under dry conditions; Wisura ZO 3368 was applied as lubricant. The method of applying the lubricant was overflowing the forming die samples before the first stroke of every experiment, which represents conditions similar to actual rotary swaging. After every experiment optical inspection was carried out on the forming die samples to determine potential wear. Neither adhesive or abrasive wear, nor plastic deformation of the macroscopic structures was found
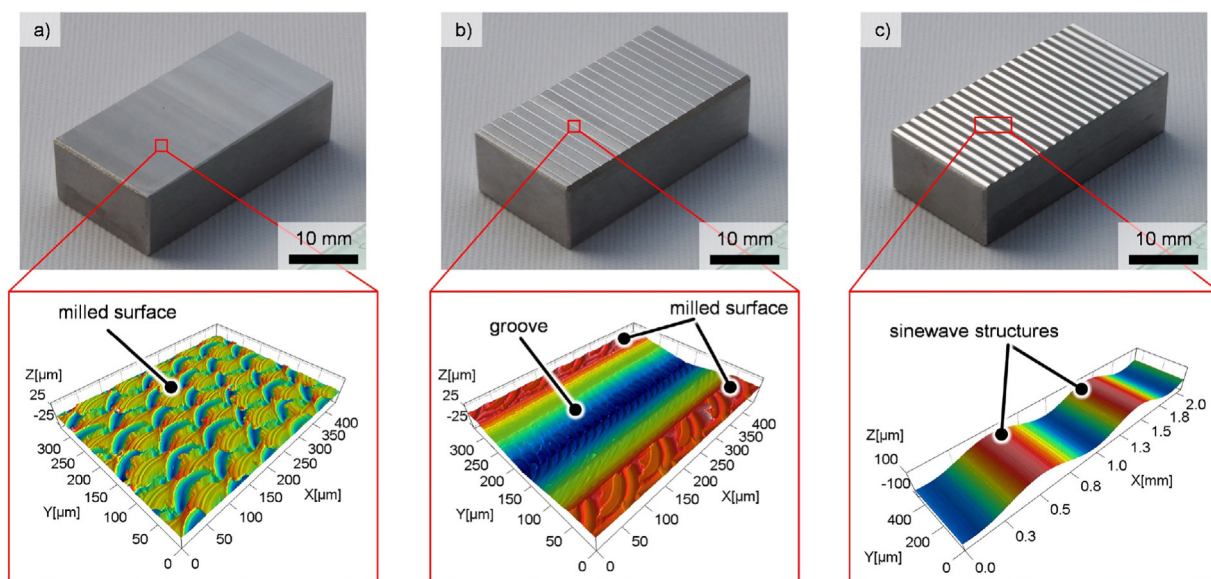

Fig. 8. Structured forming die samples and attributed surface plots; a) microstructured forming die sample (arithmetical mean height Sa = 1155 nm), b) forming die sample with mesoscopic grooves (groove depth 18 µm, groove pitch 1.5 mm), and c) forming die sample with sinewave macroscopic surface structure (wavelength λ = 1.3 mm, amplitude A = 0.05 mm).

Table 1
Forming die samples.

Sample	Structure dimension	Groove pitch – [mm]	Groove depth – [μm]	Groove width – [μm]	Amplitude A [mm]	Areal roughness Sa [nm]
R	–	–	–	–	–	24
#1	Micro	–	–	–	–	1155
#2a	Meso	1.5	45.5	247.3	–	656
#2b	Meso	1.0	42.3	252.0	–	1150
#2c	Meso	0.5	18.6	237.4	–	920
#3a	Macro	–	–	–	0.03	143
#3b	Macro	–	–	–	0.04	194
#3c	Macro	–	–	–	0.05	127

for any of the samples for both, the lubricated and the dry experiments.

Results and discussion

The results of the experiments carried out under lubricated conditions are displayed in Fig. 9 for both, the first and the second stroke applied to the samples. As expected, for all experiments the measured forces in excitation direction $F_{R''}$ were less than the nominal excitation force $F_{R'}$. This is attributed to the transfer of the impact's energy to forming work applied to the work piece samples. The polished reference sample R provoked by far the highest horizontal reaction forces $F_{A'}$ in the lubricated experiment with 40.49 kN (first stroke) and 34.48 kN (second stroke), respectively. This can be explained encountering two effects linked to the surface design of the polished reference sample: hydrodynamic separation and no sample interlocking. Its sluggishness prevented the lubricant from flowing out the area of tribological contact during the short duration of the experiment. This resulted in a predominantly hydrodynamic separation of both the samples, associated with considerably high horizontal reaction forces. This effect was amplified by the absence of any surface structure or texture on the reference forming die sample, which could serve as a lubricant drainage. The absence of structures on the reference forming die sample's surface, furthermore, prevented from any interlocking of the samples, which is associated with an increase of friction or a decrease of the horizontal reaction force $F_{A'}$, respectively.

The micro structured sample #1 provoked an about 30% lower horizontal reaction force $F_{A'}$ with 33.44 kN for the first stroke and 19.63 kN for the second stroke in the lubricated experiment compared to those measured for the polished reference sample. Again, hydrodynamic separation of the samples during the experiment is expected to be the main effect governing the frictional conditions. The slightly lower horizontal reaction forces

are attributed to a loss in hydrodynamic pressure of the lubricant, especially at the border of the area of tribological contact between forming die and work piece sample. The more "open" micro structure design, here, acts as a lubricant drainage, rather than maintaining hydrodynamic pressure known from surfaces exhibiting "closed" or pocket like structures. This ultimately leads to an increase of the contact area between the solid sample bodies on microscopic level and thus to a change in frictional conditions associated with higher frictional forces or a lower horizontal reaction force $F_{A'}$, respectively. A sample interlocking caused by the imprinting of the softer work piece sample material into the micro structured surface of the sample #1 and thus a contribution to the frictional force is not expected here, as a change in surface finish of the work piece sample could not be observed after the experiment. Besides, it was found for both the experiments carried out with the forming die samples R and #1, that the horizontal reaction force measured for the second stroke is less than that of the first stroke. This is assigned to a loss of lubricant quantity in the area of tribological contact between the samples after the first stroke. This also leads to an increase of solid–solid contact area of both the forming die sample and the work piece sample on microscopic level and therefore an increase of friction.

In all experiments under lubricated conditions applying forming dies samples exhibiting mesoscopic and macroscopic surface structures distinctively less horizontal reaction forces $F_{A'}$ were measured. For the sample #2c (mesoscopic, groove pitch = 0.5 mm) the least horizontal reaction force was found with 3.68 kN, which is less than a tenth of that measured for the polished reference forming die sample. The results are attributed to a fundamental change in contact conditions of the samples and thereby the dominant frictional mechanism. During the experiments, the softer work piece sample material is imprinted into the surface structure's cavities of the forming die samples due to present high pressures per unit area. This leads to an interlocking of both the samples. A progress in relative movement of the work piece sample in horizontal
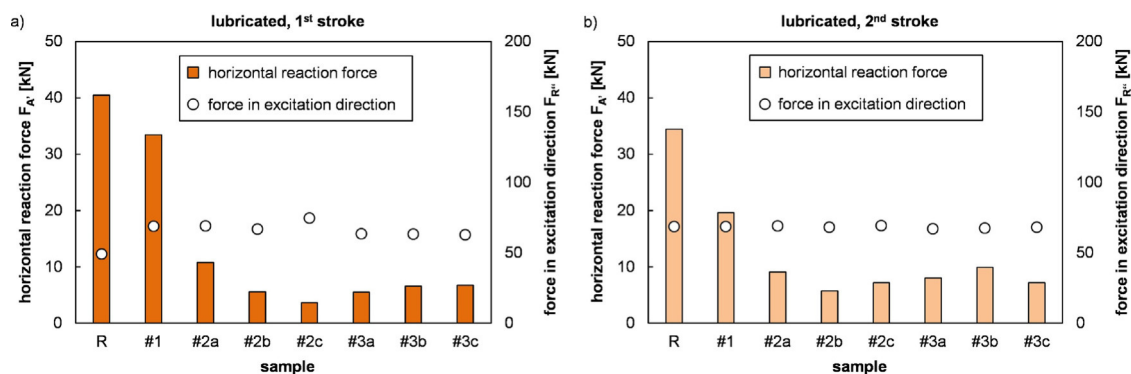

Fig. 9. Calculated horizontal reaction force $F_{A'}$ and force in excitation direction $F_{R''}$ for lubricated experiments in dependence on the sample under test; a) for first stroke, b) for second stroke.

direction mandatorily requires for a progressive plastic deformation of the work piece sample material on microscopic level associated with energy consumption and thus an increase of frictional forces. In contrast, hydrodynamic separation can be neglected in the experiments with mesoscopic and macroscopic forming die samples. Their distinct surface structures do not allow the formation of a greater area of lubricant film required for hydrodynamic separation. The samples exhibiting the mesoscopic surface structures are supposed to more effectively increase friction and reduce the horizontal reaction forces than those forming die samples with the macroscopic sinewave structures. This is explained by the comparably low amount of work piece sample material that needs to be imprinted into the grooves aligned perpendicular to the longitudinal direction, already provoking an adequate interlocking of the samples and thus a considerable increase in friction. Furthermore it is assumed, that the groove pitch has an impact on the horizontal reaction force $F_{A'}$ towards a decrease for lower numbers of groove pitch. However, at this stage the assumption cannot be clearly underlined, due to the indifferent result of the horizontal reaction force $F_{A'}$ measurement for the second stroke. With regard to the macro structured samples, no clear correlation of amplitude and the measured horizontal reaction force can be derived from the experimental results.

The results of the experiments carried out under dry conditions are displayed in Fig. 10 for both, the first and the second stroke applied to the samples. Again, for all experiments the measured forces in excitation direction $F_{R''}$ were less than the nominal excitation force $F_{R'}$, which is traced back to the forming work applied to the work piece samples. Furthermore, according to expectations, the measured horizontal reaction forces in the dry experiments, regardless of the sample type applied, were far less compared to those derived from the experiments under lubricated conditions. Measured forces barely exceeded 1 kN, what is less than a fortieth compared to the lubricated experiments.

The maximum horizontal reaction force was measured for the reference sample R at the first stroke with $F_{A'}$ = 2.13 kN. The second stroke applied to that sample resulted in a horizontal reaction force of just 0.76 kN. This finding could be linked to adhesion effects occurring in dry tribological contact. The optical inspection of the polished reference sample revealed small amounts of the work piece sample's material adhered to the smooth surface of the sample, obviously caused by cold welding. During the second stroke these welds were source of increased friction in the second stroke of the experiment. This is due to both, a scratching of the welds in the surface of the work piece sample and amplified adhesion effects.

The horizontal reaction force measured for the micro structured forming die sample #1 remained completely unchanged for first and second stroke with 0.77 kN. Remarkably, the optical inspection of the sample #1 did not revealed any work piece sample material

adhesions on its surface, what agrees well with the constant tribological conditions found for the first and second stroke of the experiment. Regarding the friction mechanism occurring for the micro structured sample, it is expected that the friction in dry tribological contact is only determined by the interactions of both the solid bodies on microscopic level. Adhesion or interlocking only play a negligible role.

The mesoscopic samples #2a to #2c provoked the lowest horizontal reaction forces for all the experiments carried out under dry conditions ranging from $F_{A'}$ = 0.47 kN to 0.67 kN. A dependence of the horizontal reaction force from the groove pitch cannot be derived from the experiments results. For those samples, a combination of the frictional effect explained for the forming die sample, i.e. solid–solid interaction on microscopic level, and sample interlocking caused by the imprinting of the softer work piece sample material into the surface grooves of the forming die samples is assumed here, resulting in comparably high friction.

The sinewave structured, macroscopic samples with the amplitudes A = 0.03 mm (#3a) and 0.04 mm (#3b) provoked the second highest horizontal reaction forces compared to all other dry experiments with up to $F_{A'}$ = 1.74 kN. When further increasing the amplitude of the sinewave structure to A = 0.05 mm (sample #3c) a distinct lower horizontal reaction force was measured with a maximum of $F_{A'}$ = 0.66 kN. Those results were consistent for both, the first and the second stroke. It is assumed, that for the amplitudes A = 0.03 mm and 0.04 mm the design of the sinewave structures at the given wavelength λ = 1.3 mm is not pronounced enough. This does not allow the structure's asperities to sink deep enough into the softer work piece sample material as result to the impact, causing a proper interlocking of the samples associated with an increase of friction. For the samples #3a (A = 0.03 mm) and #3b (0.04 mm) the occurring friction is expected to be only caused by the solid–solid interaction of the samples. As the area of tribological contact on microscopic level is less for the sample #3a (A = 0.03 mm) and even less for the sample #3b (0.04 mm) in direct comparison to that provoked by the micro structured sample #1, obviously friction must be less and the horizontal reaction force of greater magnitude, increasing for an increase of the amplitude from A = 0.03 mm to 0.04 mm. For the sample #3c exhibiting the sinewave structure with the highest amplitude of A = 0.05 mm an adequate imprinting of the structures into the work piece sample's surface is expected. The friction mechanism changes to sample interlocking and an increase in plastic material deformation, provoking higher friction and reduced horizontal reaction forces.

Conclusion

This work showed the successful development of a test rig for tribological investigations under impact loads. The test rig, with its
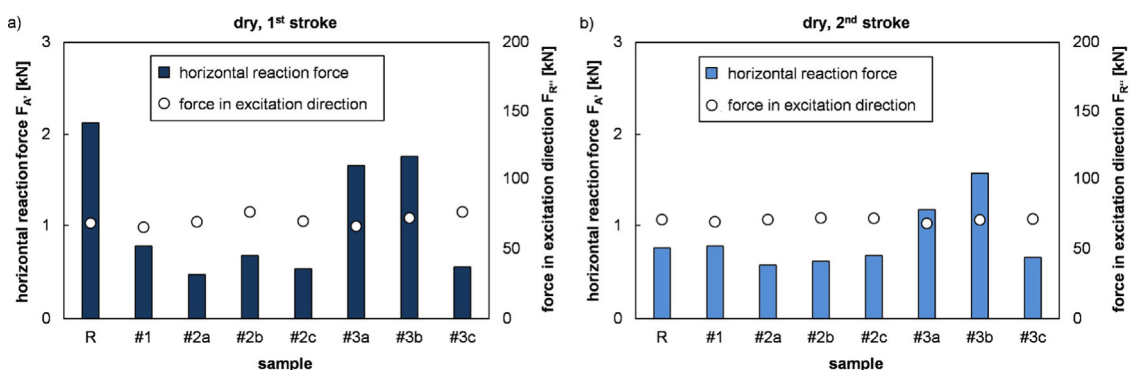

Fig. 10. Calculated horizontal reaction force $F_{A'}$ and force in excitation direction $F_{R''}$ for dry experiments in dependence on the sample under test; a) for first stroke, b) for second stroke.

solely mechanical setup, mimics typical engagement conditions of forming dies and work pieces occurring during infeed rotary swaging. It allows for the robust and process-independent tribological investigation of structured and hard coated sample surfaces, representing those of actual rotary swaging dies. Besides tribological investigations, the field of application can be extended to the durability testing of DLC coatings, e.g. through the application of excessive loads to samples provoking coating failures such as delamination. The presented tribological test rig from now on can contribute to the development of economic and ecological friendly dry bulk metal forming processes, such as dry rotary swaging.

After the designing and the setup of the test rig, tribological investigations of various samples exhibiting structured surfaces were carried out applying the test rig for tribological investigations under impact loads. Distinct differences in the tribological mechanisms provoked by different surface's design were found. In the case of lubricated experiments, polished or micro structured surfaces facilitate hydrodynamic separation of samples associated with low frictional forces. Mesoscopic structures on the samples surfaces, such as grooves, and macroscopic structures such as the investigated sinewave structures are able to distinctively reduce friction under lubricated conditions due to an interlocking of the sample's surfaces. The same investigations carried out under dry conditions generally showed an increase in friction as well as considerable different friction mechanisms. As to expectations, polished surfaces provoked adhesion and are not suitable at all for the application in dry machining. On the contrary, micro structured surfaces generated by micro milling with ball-endmills aligned normal to the machined surfaces have greatest potential to sufficiently suppress adhesion in dry tribological contact, even under harsh conditions such as high pressures per unit area typical for bulk metal forming. Mesoscopic structured surfaces are generally suitable to distinctively increase friction under dry conditions. For sinewave or macro structured surface the predominant friction mechanism is strongly dependent on structure's amplitude. Amplitudes smaller 0.05 mm reduce friction compared to the results achieved with the micro structured sample, rather than increasing friction. Only the sample surface exhibiting a sinewave structure with amplitude of 0.05 mm allowed for an adequate imprinting of the structures into the work piece sample's surface accompanied by a change of the friction mechanism towards sample interlocking. The results of the tribological investigations achieved in this work represent the basis for ongoing work regarding the surface functionalization of rotary sawing dies applied to dry rotary swaging processes.

Acknowledgements

References

[1] Vollertsen, F., Schmidt, F., 2014, Dry Metal Forming: Definition, Chances and Challenges. International Journal of Precision Engineering and Manufacturing – Green Technologyy, 1/1: 59–62.

[2] Böhmermann, F., Hasselbruch, H., Herrmann, M., Riemer, O., Mehner, A., Zoch, H.-W., Kuhfuss, B., 2015, Trockenrundkneten - Funktionalisierte Werkzeug-oberflächen für eine schmierstofffreie Prozessauslegung. wt Werkstattstechnik Online, 105/11/12: 830–835.

[3] Hasselbruch, H., Herrmann, M., Mehner, A., Zoch, H.-W., 2015, Development, Characterization and Testing Of Tungsten Doped DLC Coatings for Dry Rotary Swaging. MATEC Web of Conferences, 21: 08012-1–08012-7.

[4] Herrmann, M., Hasselbruch, H., Böhmermann, F., Kuhfuss, B., Zoch, H.-W., Mehner, A., Riemer, O., 2015, Dry Rotary Swaging. Dry Metal Forming OAJ FMT, 1:96–102.

[5] Groche, P., Heislitz, F., 2000, Kraftbedarf beim Kaltrundkneten — Abschluss-bericht zum FKM-Vorhaben Nr. 224. FKM-Heft 224.

[6] Ebrahimi, R., Najafizadeh, A., 2004, A New Method for Evaluation of Friction in Bulk Metal Forming. Journal of Materials Processing Technology, 152/2: 136–143.

[7] Spur, G., Stöferle, T., 1983, Handbuch der Fertigungstechnik Band 2/1 Umformen. Carl Hanser Verlag.

[8] Böhmermann, F., Riemer, O., 2017, Abrasive Particle Generation in Dry Rotary Swaging. Dry Metal Forming OAJ FMT, 3:1–6.

[9] Popp, U., Engel, U., 2006, Microtexturing of Cold-forging Tools — Influence on Tool Life. Proceedings of the Institution of Mechanical Engineers Part B: Journal of Engineering Manufacture, 220:27–33.

[10] Arentoft, M., Bay, N., Tang, P.T., Jensen, J., 2009, A New Lubricant Carrier for Metal Forming. CIRP Annals-Manufacturing Technology, 58/1: 243–246.

[11] Brinksmeier, E., Riemer, O., Twardy, S., 2010, Tribological Behavior of Micro Structured Surfaces for Micro Forming Tools. International Journal of Machine Tools and Manufacture, 50/4: 425–430.

[12] Böhmermann, F., Riemer, O., 2016, Tribological Performance of Textured Micro Forming Dies. Dry Metal Forming OAJ FMT, 2:067–071.

[13] Kayaba, T., Hokkirigawa, K., Kato, K., 1986, Analysis of the Abrasive Wear Mechanism by Successive Observations of the Wear Processes in a Scanning Electron Microscope. Wear, 110:419–430.

[14] Suh, N.P., Saka, N., 1987, Surface Engineering. CIRP Annals-Manufacturing Technology, 36/1: 403–407.

[15] Franzen, V., Witulski, J., Brosius, A., Trompeter, M., Tekkaya, A., 2010, Textured Surfaces for Deep Drawing Tools by Rolling. International Journal of Machine Tools and Manufacture, 50/11: 969–976.

[16] Birkert, A., Haage, S., Straub, M., 2013, Umformtechnische Herstellung komplexer Karosserieteile — Auslegung von Ziehanlagen. Springer-Verlag.

[17] Brosius, A., Mousavi, A., 2016, Lubricant Free Deep Drawing Process by Macro Structured tools. CIRP Annals-Manufacturing Technology, 65/1: 253–256.

[18] Herrmann, M., Schenck, C., Kuhfuss, B., 2016, Dry Rotary Swaging with Structured Tools. Procedia CIRP, 40:653–658.

[19] Wanheim, T., Bay, N., Petersen, A., 1974, A Theoretically Determined Model for Friction in Metal Working Processes. Wear, 28:251–258.

[20] Herrmann, M., Kuhfuß, B., Schenck, C., 2015, FEM Simulation of Infeed Rotary Swaging with Structured Tools. MATEC Web of Conferences, 21: 12003-1–12003-7.

[21] Cross, R., 1999, The Bounce of a Ball. American Journal of Physics, 67/3: 222–227.

[22] Herrmann, M., Hasselbruch, H., Böhmermann, F., Kuhfuss, B., Zoch, H.-W., Mehner, A., Riemer, O., 2015, Potentials of Dry Rotary Swaging. Dry Metal Forming OAJ FMT, 1:63–71.

[23] Vehmeyer, J., Piotrowska-Kurczewski, I., Böhmermann, F., Riemer, O., Maaß, P., 2015, Least-squares Based Parameter Identification for a Function-related Surface Optimisation in Micro Ball-end Milling. Procedia CIRP, 31:276–281.